

## Characterization of carbon dots synthesized from plant-based extracts via the hydrothermal method

Fatah Ari Kusuma Wardana<sup>1</sup> Chlara Naren Maharani<sup>1</sup> Aliffia Widyasari Putri Arbi<sup>2</sup> Mohammad Arya Zandi F.<sup>1</sup> Rizky Aflaha<sup>2,✉,✉</sup>

<sup>1</sup>Department of Physics Education, Faculty of Mathematics and Natural Sciences, Universitas Negeri Yogyakarta, Karangmalang, Yogyakarta 55281, Indonesia

<sup>2</sup>Department of Physics, Faculty of Mathematics and Natural Sciences, Universitas Gadjah Mada, Sekip Utara, BLS 21, Yogyakarta 55281, Indonesia

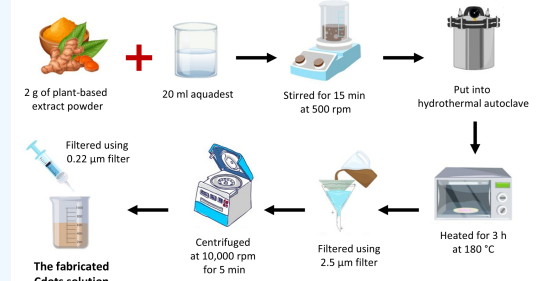
✉ Corresponding author: rizkyafaha@mail.ugm.ac.id (RA)

ARTICLE HISTORY:  Received: July 19, 2025 |  Revised: October 24, 2025 |  Accepted: October 31, 2025

### ABSTRACT

Cdots are carbon-based nanoparticles and luminescent materials that are safe for humans and the environment, and also have many potential applications. Natural precursors using local plants can be utilized, and a green synthesis approach can be used to fabricate Cdots that are advantageous in terms of sustainability, availability, low cost, and minimal toxic waste. In this study, the hydrothermal method was chosen because the process is simple, does not require a catalyst, and is suitable for natural materials. The fabricated Cdots from various plant-based extract precursors using the hydrothermal method are investigated for the chemical and optical property changes that occur during the conversion of natural extracts into Cdots. Fourier-transform infrared (FTIR) spectra show that functional groups such as O–H and C=C remain present after the Cdots synthesis process. The UV-Vis spectra show a shift in the absorption band, indicating the formation of  $sp^2$  aromatic domains and  $\pi-\pi^*$  transition in the Cdots structure, compared to plant-based extracts. Field emission scanning electron microscope (FE SEM) images show that the fabricated Cdots have a size of about  $(57 \pm 12)$  nm. These results show great potential of local plants as a base material for producing Cdots that can be beneficial for various applications.

**Keywords:** Cdots; plant-based; extract; hydrothermal



### 1. INTRODUCTION

The demand for environmentally friendly luminescent materials continues to increase, in line with the development of technologies that require alternatives to heavy metal-based compounds [1, 2]. Heavy metal-based quantum dots, such as cadmium-based materials, although known for their excellent optical performance, are also associated with toxicity [3–5], high production cost [6], and environmental hazards [7], thus limiting their wider applications. This is driving the exploration of new materials that are not only optically efficient but also safe for humans and the environment.

A promising alternative material is carbon dots (Cdots). Cdots are carbon-based nanoparticles with extremely small sizes [8]. Cdots exhibit unique fluorescent properties [9], high stability [10], as well as good biocompatibility and low toxicity [11]. Compared to conventional carbon materials, Cdots have an advantage due to the quantum confinement effect [12, 13], a physical phenomenon that enables bright fluorescence emission even in complex environments [9]. These characteristics make Cdots highly promising for various applications, including biosensing [8], bioimaging [14], heavy metal ion detection [15], catalysis [16], and applications in the energy and environmental fields [17].

The development of Cdots has also aligned with the in-

creasing adoption of green synthesis strategies. This approach emphasizes the use of plant-based extracts as a source of carbon, which are renewable [18], easily obtainable [19], low-cost [20], and produce less waste compared to synthetic chemicals [21]. These natural sources are not only abundant and cost-effective, but also often contain bioactive compounds such as flavonoids [16], phenols [22], and alkaloids [17, 23], which may contribute to enhanced chemical and optical properties of the fabricated Cdots. This study has specifically compared seven types of natural materials with different phytochemical characteristics, unlike previous studies that generally used only one type of natural material. This approach provides a comprehensive overview of the effect of precursor chemical composition on the formation of  $sp^2$  domains and the optical properties of Cdots. Thus, this study focuses not only on environmentally friendly synthesis but also on understanding the relationship between the type of natural material and the optical performance of the fabricated Cdots.

Several methods have been developed for the synthesis of Cdots. There are two primary approaches to synthesizing Cdots: top-down and bottom-up. Top-down approaches, such as laser ablation [24, 25] and electrochemical oxidation [26], often require sophisticated equipment, high energy

consumption, complex procedures, and, in several cases, hazardous chemicals [27, 28]. In contrast, bottom-up approaches, such as solvothermal, hydrothermal, and microwave-assisted synthesis [29–31], have emerged as simpler, more economical, and environmentally friendly options. For example, the hydrothermal method has been proven to be efficient [16], cost-effective [32], and environmentally friendly [32, 33]. This method allows for the conversion of natural precursors into Cdots under mild conditions, without the need for catalysts or harsh reagents, and has been shown to produce Cdots with good stability and fluorescence performance [17, 34].

In this study, Cdots were synthesized from various plant-based extracts using the hydrothermal method. The primary objective is to investigate the chemical and optical property changes that occur during the conversion of natural extracts into Cdots. Characterization was conducted using Fourier-transform infrared (FTIR) spectroscopy to identify the transformation of functional groups, UV-Vis spectrophotometry to observe the absorbance features associated with Cdots formation, and a field emission scanning electron microscope (FE SEM) to observe the size distribution of fabricated Cdots. This work highlights the potential of simple, green hydrothermal synthesis using natural precursors to produce functional carbon nanomaterials.

## 2. MATERIALS AND METHODS

### 2.1 Materials

Plant-based extract powders, including *Clitoria ternatea*, *Curcuma longa*, *Annona muricata* L., *Allium sativum*, *Moringa oleifera* L., *Psidium guajava* L., and *Zingiber officinale*, were obtained from Bigfood Production, Indonesia. Aquadest was purchased from Jaya Santosa, Indonesia. Filters with a size of 0.22 µm and 2.5 µm were products from Microlab Scientific, China, and Whatman, United Kingdom, respectively. Fourier-transform infrared spectroscopy (FTIR, 8201 PC, Shimadzu) and ultraviolet-visible spectroscopy (UV-Vis, Spectrophotometer UV-1900, Shimadzu) were used to characterize the fabricated samples.

### 2.2 Cdots fabrication process

Cdots were synthesized using a bottom-up hydrothermal method with plant-based extract powders serving as carbon precursors. A total of 2 grams of each selected plant-based extract powder was accurately weighed and dispersed into 20 mL of aquadest. The mixture was stirred at 500 rpm for 30 minutes to ensure a homogeneous suspension. The suspension was then transferred into a PTFE-lined Teflon vessel and sealed within a stainless steel autoclave reactor. The sealed reactor was placed in a laboratory furnace and heated at 180 °C for 3 hours to initiate hydrothermal carbonization. During this stage, the high-temperature and high-pressure aqueous environment promotes the breakdown of complex biomolecules and the formation of carbonaceous nanoparticles. After the reaction, the autoclave was allowed to cool naturally to room temperature.

The product obtained from the hydrothermal process was a brownish colloidal suspension accompanied by black solid residues, indicating the partial conversion of organic material into carbon nanoparticles. Initial purification was carried out by filtering the suspension using a 2.5 µm filter paper to separate the larger aggregates and residual solids. The resulting filtrate was then subjected to centrifugation at 10,000 rpm for 5 minutes to further remove suspended particles. The supernatant obtained was subsequently passed

**Table 1.** List of sample types and corresponding solution labels used for characterization.

Sample type	Solution sample information	Sample label
Plant-based extract solution	<i>Clitoria ternatea</i>	CT
	<i>Curcuma longa</i>	CL
	<i>Annona muricata</i> L.	AM
	<i>Allium sativum</i>	AS
	<i>Moringa oleifera</i> L.	MO
	<i>Psidium guajava</i> L.	PG
Cdots solution	<i>Zingiber officinale</i>	ZO
	<i>Clitoria ternatea</i>	CTc
	<i>Curcuma longa</i>	CLc
	<i>Annona muricata</i> L.	AMc
	<i>Allium sativum</i>	ASc
	<i>Moringa oleifera</i> L.	MOc
	<i>Psidium guajava</i> L.	PGc
	<i>Zingiber officinale</i>	ZOc

through a 0.22 µm syringe filter to isolate fine-sized carbon dots and eliminate any remaining particulate contaminants. The final Cdots solution was stored in a clean container and kept at a temperature of 10 °C for further characterization.

For FTIR testing, the plant-based extract and Cdots solution were tested as-is. Meanwhile, for UV-Vis analysis, the solution was diluted at a ratio of 1:40 with aquadest to facilitate observation. For FE SEM imaging, the sample was dried at 60 °C for 30 minutes. The fabrication process of the Cdots solution is shown in Figure 1, while the obtained solutions for characterization are listed in Table 1.

## 3. RESULTS AND DISCUSSION

### 3.1 Chemical and morphological characterization

Figure 2a presents the FTIR spectrum of the plant-based extract solution before the hydrothermal process. The spectrum shows a broad transmittance band in the range of 3220–3380 cm<sup>-1</sup>, centered at approximately 3330 cm<sup>-1</sup> for each extract solution. This peak indicates the presence of O–H stretching vibrations, a characteristic feature of hydroxyl groups typically present in polyphenols, flavonoids, and other plant-derived compounds [35, 36]. This band suggests the abundance of hydrogen-bonded hydroxyl groups in the natural precursor. In addition, a sharp peak around 1635 cm<sup>-1</sup> is observed, indicating C=C stretching vibrations from aromatic structures or unsaturated carbon frameworks, which are also commonly found in phytochemicals [37]. On the other hand, Figure 2b shows the FTIR spectrum of the resulting Cdots solutions after the hydrothermal process. Notably, the spectrum exhibits similar transmittance features, particularly the broad O–H stretching peak near 3331 cm<sup>-1</sup> and the C=C stretching peak around 1635 cm<sup>-1</sup>, both of which are clearly visible. The absence of significant peak shifts or new bands suggests that the hydrothermal process did not drastically influence the primary functional groups present in the original extract.

The spectral similarity between the precursor solution and the Cdots solution could be twofold. First, it suggests that the carbonization process may have occurred through mild dehydration and condensation reactions, which are sufficient to induce the nucleation of carbonized domains without total degradation of the original biomolecules [38, 39]. Secondly, it

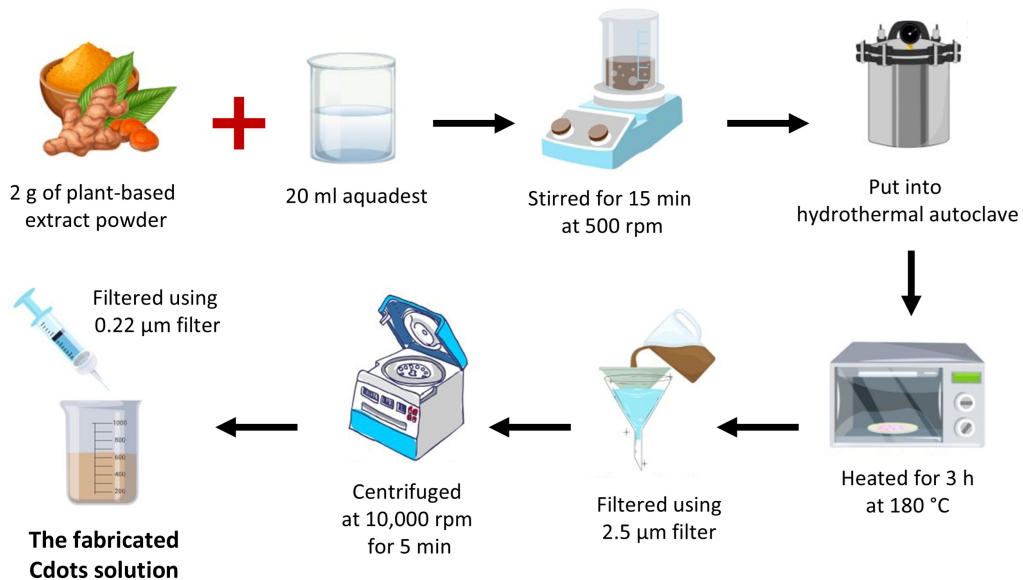


**Figure 1.** Fabrication process of Cdots from plant-based extract powder.

suggests that certain bioactive groups, such as phenolic -OH groups and conjugated C=C structures, remain partially retained on the surface of Cdots, possibly as surface-anchoring ligands [38, 39].

The unchanged functional groups on the fabricated Cdots solutions are potentially beneficial. Hydroxyl and aromatic groups on the surface of Cdots can improve dispersibility in water, provide reactive sites for further functionalization, and contribute to antioxidant or antimicrobial properties [40–42]. In addition, such surface chemistry is particularly advantageous for biological applications, where interactions with proteins or cell membranes often rely on hydrogen bonding or  $\pi$ - $\pi$  interactions [43]. Although the FTIR spectra do not show drastic transformations, the consistency of the peaks supports the hypothesis that hydrothermal synthesis induces nanostructures and partial carbonization, rather than full decomposition of precursor molecules.

Figure 2c shows the morphological measurement results of the evaporated CLc sample at 60 °C on an aluminum foil using FE-SEM. The CLc morphology shows a relatively homogeneous surface without any indication of aggregation, with an average particle size of  $(57.4 \pm 12.3)$  nm. This size indicates that the hydrothermal process successfully converted the precursor into nano-scale particles, supporting the successful fabrication of Cdots. Surface element analysis showed that carbon (C) and oxygen (O) atoms dominated with percentages of  $(50.57 \pm 0.37)\%$  and  $(43.91 \pm 0.59)\%$ , respectively, in line with FTIR results confirming the presence of O-H and C=C groups on the Cdots surface.

### 3.2 UV-Vis measurement

The UV-Vis spectra of plant-based extract solutions (i.e., CT, CL, AM, AS, MO, PG, and ZO) before hydrothermal processing are displayed in Figure 3a. Absorption peaks in the range of 254–279 nm were observed in several extract solutions, including CT, AM, AS, and MO, indicating the presence of the  $\pi$ - $\pi^*$  transition of aromatic  $sp^2$  groups [44]. This transition is usually associated with phenolic structures or other aromatic compounds commonly found in plant extracts. In CT, two small peaks around 574 nm and 619 nm were also

observed, which refer to the spectrum of anthocyanins [45], natural pigment compounds commonly found in blue or purple flowers. According to a previous study, a small peak in the PG spectrum at about 309 nm suggested the presence of flavonoids [46]. The lack of chromophores in CL and ZO, on the other hand, may have contributed to their inability to display a distinct absorption peak.

After the hydrothermal process, the resulting Cdots solutions showed significant changes in the UV-Vis spectra, as displayed in Figure 3b. All samples exhibit a characteristic absorbance peak around 279–283 nm, which is indicative of the  $\pi$ - $\pi^*$  transition of aromatic  $sp^2$  domains [47]. This distinct peak, differing from the original extract spectra, suggests that a transformation of chemical structure occurred during the synthesis. The shift in peak shape and intensity provides early evidence that the Cdots fabrication process was successful.

The absorption peaks in the Cdots samples are more intense and sharper than those in the extracts, implying that partial carbonization during the hydrothermal process led to the formation of extended  $\pi$ -conjugated systems and larger  $sp^2$  domains. This reorganization enhances the optical characteristics and absorbance of the Cdots [48, 49]. In addition to confirming Cdots formation, a qualitative comparison of various plant precursors was conducted. Among all samples, CLc showed the most prominent absorption peak in the 279–283 nm range. This strong peak correlates with blue-green luminescence under. In addition, the appearance of a peak at 218 nm in the CLc sample indicates the possible presence of aliphatic carbon chains or short groups resulting from partial decomposition [16, 50]. These peaks also support the FTIR spectra that show the presence of C=C and O-H groups, which may remain on the surface of Cdots.

Overall, the shift in the UV-Vis spectra between the Cdots solution and the plant-based extract solution provides compelling evidence that the hydrothermal synthesis method used in this work creates new structures with unique optical properties distinct from the original material. As documented in previous studies, Cdots are also a promising option for optoelectronic, fluorophore, and photoconductor applications

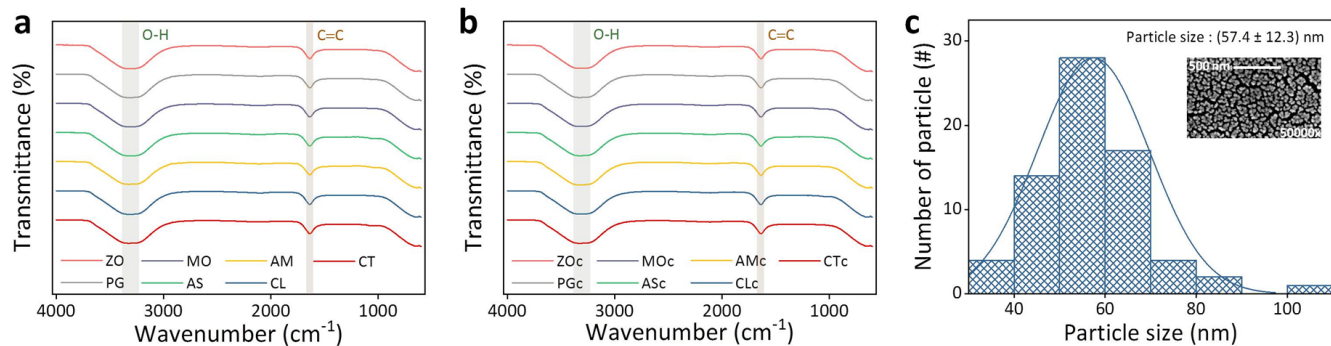


**Figure 2.** (a) FTIR spectra of plant-based extract solution as base material for producing Cdots. (b) FTIR spectra of the fabricated Cdots solution. (c) Particle size distribution measurement and SEM image of the CLc sample.

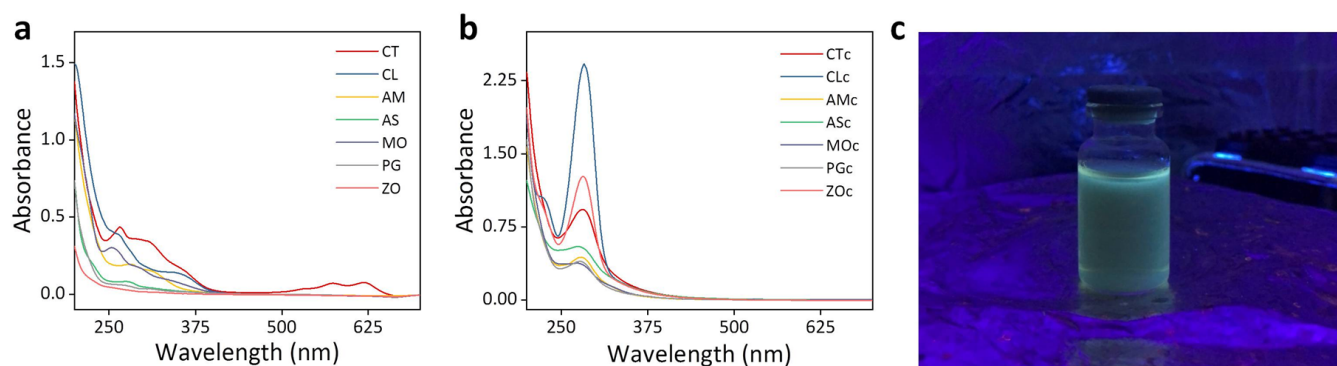


**Figure 3.** (a) UV-Vis spectra of plant-based extract solutions. (b) UV-Vis spectra of the fabricated Cdots solutions. (c) CLc luminescence photograph in a UV box.

due to the increase in  $\pi$ -conjugation and reorganization of the aromatic structure [51].

The result of the liquid CLc sample photograph inside a UV box is shown in Figure 3c. It can be seen that the sample emits a blue-green luminescence when exposed to UV light. This phenomenon indicates that the CL sample, having undergone hydrothermal processing, has successfully formed luminescent material—one of the characteristic features of Cdots.

#### 4. CONCLUSION

This study successfully synthesized Cdots from various plant extract powders through the hydrothermal method using a green synthesis approach. Characterization results show that the Cdots formed retain the main active functional groups, such as O-H and C=C, as confirmed through FTIR spectra. In addition, UV-Vis analysis revealed changes in the optical absorption pattern in the range of 279–283 nm, which is typical for the aromatic sp<sup>2</sup> domain, indicating the formation of conjugated carbon structures and supporting the successful formation of Cdots. The observed changes in chemical and optical characteristics indicate that the hydrothermal process is not only simple and environmentally friendly, but also effective in producing Cdots from plant-based extracts. Although the characterization performed in this study is still limited to FTIR, UV-Vis, and FE-SEM, the results provide a strong initial foundation for the further development of

natural extract-based Cdots, especially for applications in the environmental, sensing, and biomedical fields. However, this study serves as an initial screening rather than a definitive determination of the most superior precursor. Therefore, only qualitative analysis was used to compare the chemical and optical changes in the fabricated Cdots from different plant extracts. Further research will include quantitative evaluations, such as photoluminescence intensity, quantum yield, and surface charge analysis, to provide a more comprehensive comparison between precursors and identify the most promising plant sources for future applications.

#### CRedit AUTHOR STATEMENT

FAKW: Conceptualization, Investigation, Writing – Original Draft, Writing – Review & Editing. CNM: Writing – Original Draft, Writing – Review & Editing. AWPA: Investigation, Writing – Original Draft. MAZF: Investigation. RA: Conceptualization, Investigation, Writing – Review & Editing, Supervision. All authors confirmed the final manuscript.

#### DATA AVAILABILITY STATEMENT

The datasets generated during and/or analyzed during the current study are available from the corresponding author on reasonable request.

## CONFLICT OF INTEREST

The authors declare that there are no conflicts of interest associated with this publication, and there has been no significant financial support for this work that could have influenced its outcome.

## ACKNOWLEDGMENTS

The authors thank all Taste and Odor Research Center (TORC) Universitas Gadjah Mada members who have provided technical support in this presented research work.

## REFERENCES

- [1] Q. Gong, H. Chun Wong, J. Chen, P. Li, L. Lu, Solar-driven adaptive radiative cooling coating with polymer carbon dots-enhanced photoluminescence for urban skin, *Chemical Engineering Journal* 494 (2024) 153262. <https://doi.org/10.1016/j.cej.2024.153262>.
- [2] J. Sobhannan, J. V. Rival, A. Anas, E. Sidharth Shibu, Y. Takano, V. Biju, Luminescent quantum dots: Synthesis, optical properties, bioimaging and toxicity, *Advanced Drug Delivery Reviews* 197 (2023) 114830. <https://doi.org/10.1016/j.addr.2023.114830>.
- [3] L. Hu, H. Zhong, Z. He, Toxicity evaluation of cadmium-containing quantum dots: A review of optimizing physico-chemical properties to diminish toxicity, *Colloids and Surfaces B: Biointerfaces* 200 (2021) 111609. <https://doi.org/10.1016/j.colsurfb.2021.111609>.
- [4] D. Mo, L. Hu, G. Zeng, G. Chen, J. Wan, Z. Yu, Z. Huang, K. He, C. Zhang, M. Cheng, Cadmium-containing quantum dots: properties, applications, and toxicity, *Applied Microbiology and Biotechnology* 101 (2017) 2713–2733. <https://doi.org/10.1007/s00253-017-8140-9>.
- [5] K. G. Li, J. T. Chen, S. S. Bai, X. Wen, S. Y. Song, Q. Yu, J. Li, Y. Q. Wang, Intracellular oxidative stress and cadmium ions release induce cytotoxicity of unmodified cadmium sulfide quantum dots, *Toxicology in Vitro* 23 (2009) 1007–1013. <https://doi.org/10.1016/j.tiv.2009.06.020>.
- [6] M. Fu, K. Critchley, Inkjet printing of heavy-metal-free quantum dots-based devices: a review, *Nanotechnology* 35 (2024) 302002. <https://doi.org/10.1088/1361-6528/ad40b3>.
- [7] L. Geng, H. Wang, M. Liu, J. Huang, G. Wang, Z. Guo, Y. Guo, X. Sun, Research progress on preparation methods and sensing applications of molecularly imprinted polymer-aptamer dual recognition elements, *Science of The Total Environment* 912 (2024) 168832. <https://doi.org/10.1016/j.scitotenv.2023.168832>.
- [8] M. Pourmadadi, E. Rahmani, M. Rajabzadeh-Khosroshahi, A. Samadi, R. Behzadmehr, A. Rahdar, L. F. R. Ferreira, Properties and application of carbon quantum dots (cqds) in biosensors for disease detection: A comprehensive review, *Journal of Drug Delivery Science and Technology* 80 (2023) 104156. <https://doi.org/10.1016/j.jddst.2023.104156>.
- [9] L. J. Desmond, A. N. Phan, P. Gentile, Critical overview on the green synthesis of carbon quantum dots and their application for cancer therapy, *Environmental Science: Nano* 8 (2021) 848–862. <https://doi.org/10.1039/D1EN00017A>.
- [10] H. E. Emam, Carbon quantum dots derived from polysaccharides: Chemistry and potential applications, *Carbohydrate Polymers* 324 (2024) 121503. <https://doi.org/10.1016/j.carbpol.2023.121503>.
- [11] B. Gidwani, V. Sahu, S. S. Shukla, R. Pandey, V. Joshi, V. K. Jain, A. Vyas, Quantum dots: Prospectives, toxicity, advances and applications, *Journal of Drug Delivery Science and Technology* 61 (2021) 102308. <https://doi.org/10.1016/j.jddst.2020.102308>.
- [12] B. Eller, C. W. Clark, Y. Wang, Scaling law of quantum confinement in single-walled carbon nanotubes, *The Journal of Chemical Physics* 162 (2025) 144303. <https://doi.org/10.1063/5.0245889>.
- [13] W. Li, X. Wang, J. Lin, X. Meng, L. Wang, M. Wang, Q. Jing, Y. Song, A. Vomiero, H. Zhao, Controllable and large-scale synthesis of carbon quantum dots for efficient solid-state optical devices, *Nano Energy* 122 (2024) 109289. <https://doi.org/10.1016/j.nanoen.2024.109289>.
- [14] A. Sangjan, S. Boonsith, K. Sansanaphongpricha, T. Thirbanmai, S. Ratchahat, N. Laosiripojana, K. C.-W. Wu, H. S. Shin, C. Sakdaronnarong, Facile preparation of aqueous-soluble fluorescent polyethylene glycol functionalized carbon dots from palm waste by one-pot hydrothermal carbonization for colon cancer nanotheranostics, *Scientific Reports* 12 (2022) 10550. <https://doi.org/10.1038/s41598-022-14704-x>.
- [15] L. Zhong, W. Liu, Z. Xie, J. Liu, Biomimetic synthesis of rpl14b-based cdse quantum dots for the detection of heavy metal copper ions, *RSC Advances* 14 (2024) 16821–16827. <https://doi.org/10.1039/D4RA02022G>.
- [16] E. K. Sari, R. M. Tumbelaka, H. Ardiyanti, N. I. Istiqomah, Chotimah, E. Suharyadi, Green synthesis of magnetically separable and reusable  $Fe_3O_4/CDots$  nanocomposites photocatalyst utilizing *Moringa oleifera* extract and watermelon peel for rapid dye degradation, *Carbon Resources Conversion* 6 (2023) 274–286. <https://doi.org/10.1016/j.crcon.2023.04.003>.
- [17] N. Nath, A. Kumar, S. Chakraborty, S. Soren, A. Barik, K. Pal, F. G. J. de Souza, Carbon nanostructure embedded novel sensor implementation for detection of aromatic volatile organic compounds: An organized review, *ACS Omega* 8 (2023) 4436–4452. <https://doi.org/10.1021/acsomega.2c05953>.
- [18] P. Dhumal, S. Chakraborty, B. Ibrahim, M. Kaur, E. Valsamis-Jones, Green-synthesised carbon nanodots: A swot analysis for their safe and sustainable innovation, *Journal of Cleaner Production* 480 (2024) 144115. <https://doi.org/10.1016/j.jclepro.2024.144115>.
- [19] M. M. Rahman, M. Maniruzzaman, M. S. Yeasmin, A state-of-the-art review focusing on the significant techniques for naturally available fibers as reinforcement in sustainable biocomposites: Extraction, processing, purification, modification, as well as characterization study, *Results in Engineering* 20 (2023) 101511. <https://doi.org/10.1016/j.rineng.2023.101511>.
- [20] V. Bressi, A. M. Balu, D. Iannazzo, C. Espro, Recent advances in the synthesis of carbon dots from renewable biomass by high-efficient hydrothermal and microwave green approaches, *Current Opinion in Green and Sustainable Chemistry* 40 (2023) 100742. <https://doi.org/10.1016/j.cogsc.2022.100742>.
- [21] J. A. Abdalla, R. A. Hawileh, A. Bahurudeen, G. Jyothsna, A. Sofi, V. Shanmugam, B. S. Thomas, A comprehensive review on the use of natural fibers in cement/geopolymer concrete: A step towards sustainability, *Case Studies in Construction Materials* 19 (2023) e02244. <https://doi.org/10.1016/j.cscm.2023.e02244>.
- [22] W. Liu, X. Cui, Y. Zhong, R. Ma, B. Liu, Y. Xia, Phenolic metabolites as therapeutic in inflammation and neoplasms: Molecular pathways explaining their efficacy, *Pharmacological Research* 193 (2023) 106812. <https://doi.org/10.1016/j.phrs.2023.106812>.
- [23] X. Yang, X. Miao, L. Dai, X. Guo, J. Jenis, J. Zhang, X. Shang, Isolation, biological activity, and synthesis of isoquinoline alkaloids, *Natural Product Reports* 41 (2024) 1652–1722. <https://doi.org/10.1039/D4NP00023D>.
- [24] M. Bulla, V. Kumar, R. Devi, S. Kumar, R. Dahiya, P. Singh, A. K. Mishra, Exploring the frontiers of carbon nanotube synthesis techniques and their potential applications in supercapacitors, gas sensing, and water purification, *Journal of Environmental Chemical Engineering* 12 (2024) 114504. <https://doi.org/10.1016/j.jece.2024.114504>.
- [25] F. Ye, K. P. Musselman, Synthesis of low dimensional nanomaterials by pulsed laser ablation in liquid, *APL Materials* 12 (2024) 50602. <https://doi.org/10.1063/5.0199104>.
- [26] D. Rocco, V. G. Moldoveanu, M. Feroci, M. Bortolami, F. Vetrica, Electrochemical synthesis of carbon quantum dots, *ChemElectroChem* 10 (2023) e202201104. <https://doi.org/10.1002/electro.202201104>.

celc.202201104.

[27] W. Fawaz, J. Hasian, I. Alghoraibi, Synthesis and physico-chemical characterization of carbon quantum dots produced from folic acid, *Scientific Reports* 13 (2023) 18641. <https://doi.org/10.1038/s41598-023-46084-1>.

[28] I.-A. Baragau, Z. Lu, N. P. Power, D. J. Morgan, J. Bowen, P. Diaz, S. Kellici, Continuous hydrothermal flow synthesis of s-functionalised carbon quantum dots for enhanced oil recovery, *Chemical Engineering Journal* 405 (2021) 126631. <https://doi.org/10.1016/j.cej.2020.126631>.

[29] A. Hebbal, R. Selvaraj, R. Vinayagam, T. Varadavenkatesan, P. S. Kumar, P. A. Duc, G. Rangasamy, A critical review on the environmental applications of carbon dots, *Chemosphere* 313 (2023) 137308. <https://doi.org/10.1016/j.chemosphere.2022.137308>.

[30] Z. Li, K. Peng, N. Ji, W. Zhang, W. Tian, Z. Gao, Advanced mechanisms and applications of microwave-assisted synthesis of carbon-based materials: a brief review, *Nanoscale Advances* 7 (2025) 419–432. <https://doi.org/10.1039/D4NA00701H>.

[31] H. Widiyandari, E. D. Pratama, H. Parasdila, R. Suryana, O. Arutanti, Y. Astuti, Synthesis of zno–cdots nanoflower by hydrothermal method for antibacterial agent and dye photodegradation catalyst, *Results in Materials* 20 (2023) 100491. <https://doi.org/10.1016/j.rinma.2023.100491>.

[32] Z. Chen, Y. Guo, L. Luo, Z. Liu, W. Miao, Y. Xia, A critical review of hydrochar based photocatalysts by hydrothermal carbonization: synthesis, mechanisms, and applications, *Biochar* 6 (2024) 74. <https://doi.org/10.1007/s42773-024-00364-9>.

[33] J. Yue, L. Li, L. Cao, M. Zan, D. Yang, Z. Wang, Z. Chang, Q. Mei, P. Miao, W.-F. Dong, Two-step hydrothermal preparation of carbon dots for calcium ion detection, *ACS Applied Materials & Interfaces* 11 (2019) 44566–44572. <https://doi.org/10.1021/acsami.9b13737>.

[34] M. Tariq, S. Shivalkar, H. Hasan, A. K. Sahoo, M. P. Sk, Manganese doping in biomass derived carbon dots amplifies white light-induced antibacterial activity, *ACS Omega* 8 (2023) 49460–49466. <https://doi.org/10.1021/acsomega.3c08586>.

[35] P. Wongsa, P. Phatikulrungsun, S. Prathumthong, Ft-ir characteristics, phenolic profiles and inhibitory potential against digestive enzymes of 25 herbal infusions, *Scientific Reports* 12 (2022) 6631. <https://doi.org/10.1038/s41598-022-10669-z>.

[36] M. Ramli, I. Sujoko, N. Adhha, D. Annas, M. Nikmatullah, H. A. Ariyanta, D. O. B. Apriandani, I. S. Saputra, K. Khairurrijal, Influence of various concentrations of chloroauric acid on the fabrication of gold nanoparticles: Green synthesis using *Elaeis guineensis* jacq leaf extract and characterizations, *Results in Surfaces and Interfaces* 17 (2024) 100317. <https://doi.org/10.1016/j.rsurfi.2024.100317>.

[37] O. P. Bolade, A. B. Williams, N. U. Benson, Dataset on analytical characterization of bioactive components from *Azadirachta indica*, *Canna indica*, *Magnifera indica* and *Moringa oleifera* leaf extracts and their applications in nanoparticles biosynthesis, *Data in Brief* 38 (2021) 107407. <https://doi.org/10.1016/j.dib.2021.107407>.

[38] A. Visheratina, L. Hesami, A. K. Wilson, N. Baalbaki, N. Noginova, M. A. Noginov, N. A. Kotov, Hydrothermal synthesis of chiral carbon dots, *Chirality* 34 (2022) 1503–1514. <https://doi.org/10.1002/chir.23509>.

[39] S. J. Mohammed, K. M. Omer, F. E. Hawaiz, Deep insights to explain the mechanism of carbon dot formation at various reaction times using the hydrothermal technique: Ft-ir,  $^{13}\text{C}$ -nmr,  $^1\text{H}$ -nmr, and uv-visible spectroscopic approaches, *RSC Advances* 13 (2023) 14340–14349. <https://doi.org/10.1039/D3RA01646C>.

[40] Q. Yang, L. Wei, X. Zheng, L. Xiao, Single particle dynamic imaging and  $\text{Fe}^{3+}$  sensing with bright carbon dots derived from bovine serum albumin proteins, *Scientific Reports* 5 (2015) 17727. <https://doi.org/10.1038/srep17727>.

[41] B. Al Farsi, R. G. S. Sofin, H. Al Shidhani, E.-S. I. El-Shafey, A. S. Al-Hosni, F. Al Marzouqi, A. Issac, A. Al Nabhani, O. K. Abou-Zied, The effect of microwave power level and post-synthesis annealing treatment on oxygen-based functional groups present on carbon quantum dots, *Journal of Luminescence* 252 (2022) 119326. <https://doi.org/10.1016/j.jlumin.2022.119326>.

[42] X. Dong, W. Liang, M. J. Meziani, Y.-P. Sun, L. Yang, Carbon dots as potent antimicrobial agents, *Theranostics* 10 (2020) 671–686. <https://doi.org/10.7150/thno.39863>.

[43] S. Miao, K. Liang, J. Zhu, B. Yang, D. Zhao, B. Kong, Heteroatom-doped carbon dots: Doping strategies, properties and applications, *Nano Today* 33 (2020) 100879. <https://doi.org/10.1016/j.nantod.2020.100879>.

[44] A. O. da Silva, M. O. Rodrigues, M. H. Sousa, A. F. C. Campos, ph-dependent surface properties of n–cdots obtained by the hydrothermal method with multicolored emissions, *Colloids and Surfaces A: Physicochemical and Engineering Aspects* 621 (2021) 126578. <https://doi.org/10.1016/j.colsurfa.2021.126578>.

[45] N. A. Ludin, M. A. M. Al-Alwani, A. B. Mohamad, A. A. H. Kadhum, N. H. Hamid, M. A. Ibrahim, M. A. M. Teridi, T. M. Ali Al-Hakeem, A. Mukhlus, K. Sopian, Utilization of natural dyes from *Zingiber officinale* leaves and *Clitoria ternatea* flowers to prepare new photosensitisers for dye-sensitised solar cells, *International Journal of Electrochemical Science* 13 (2018) 7451–7465. <https://doi.org/10.20964/2018.08.04>.

[46] E. H. Anouar, J. Gierschner, J.-L. Duroux, P. Trouillas, Uv/visible spectra of natural polyphenols: A time-dependent density functional theory study, *Food Chemistry* 131 (2012) 79–89. <https://doi.org/10.1016/j.foodchem.2011.08.034>.

[47] X. Li, L. Yan, J. Si, H. Xu, Y. Xu, Tuning the photoluminescence property of carbon dots by ultraviolet light irradiation, *RSC Advances* 9 (2019) 12732–12736. <https://doi.org/10.1039/C9RA02080B>.

[48] G. Gedda, S. A. Sankaranarayanan, C. L. Putta, K. K. Gudimella, A. K. Rengan, W. M. Girma, Green synthesis of multi-functional carbon dots from medicinal plant leaves for antimicrobial, antioxidant, and bioimaging applications, *Scientific Reports* 13 (2023) 6371. <https://doi.org/10.1038/s41598-023-33652-8>.

[49] A. Ponnusamy, G. Murugan, A. Mittal, J. Saetang, T. Prodpran, J.-W. Rhim, S. Benjakul, Carbon dots derived from polyphenols by hydrothermal carbonization: Spectral, antioxidant, and antimicrobial properties and cytotoxicity assessment, *Food Biophysics* 20 (2025) 89. <https://doi.org/10.1007/s11483-025-09983-6>.

[50] W. Meng, X. Bai, B. Wang, Z. Liu, S. Lu, B. Yang, Biomass-derived carbon dots and their applications, *Energy & Environment Materials* 2 (2019) 172–192. <https://doi.org/10.1002/eem2.12038>.

[51] Y. Yamaguchi, Y. Matsubara, T. Ochi, T. Wakamiya, Z. Yoshida, How the  $\pi$  conjugation length affects the fluorescence emission efficiency, *Journal of the American Chemical Society* 130 (2008) 13867–13869. <https://doi.org/10.1021/ja8040493>.